Synthesis, Structure, and Bonding of d^0/f^n Metallacarboranes Incorporating the η^7-Carboranyl Ligand

Kwoli Chui,[†] Qingchuan Yang,[†] Thomas C. W. Mak,[†] Wai Han Lam,[‡] Zhenyang Lin,[‡] and Zuowei Xie*,[†]

Contribution from the Departments of Chemistry, The Chinese University of Hong Kong, Shatin, New Territories, Hong Kong, and The Hong Kong University of Science and Technology, Kowloon, Hong Kong, P. R. China

Received January 18, 2000

Abstract: Treatment of 1,2-$(C_6H_5CH_2)_2$-1,2-$C_2B_{10}H_{10}$ with excess Na or Li metal in THF followed by reaction with MCl_3 in the presence of excess alkali metal gave novel 13-vertex *closo*-metallacarboranes $\{[(C_6H_5CH_2)_2C_2B_{10}H_{10}]M(THF)\}_2\{Na(THF)_3\}_2\cdot 2THF$ (M = Dy (**1**), Y (**2**), Er (**3**)) or $[\{(C_6H_5CH_2)_2C_2B_{10}H_{10}\}M(THF)]_2[Li(THF)_4]_2$ (M = Y (**5**), Er (**6**)) in moderate to good yield, respectively. Recrystallization of **3** from a DME solution afforded DME-coordinated metallacarborane $\{[(C_6H_5CH_2)_2C_2B_{10}H_{10}]Er(DME)\}_2\{Na(DME)_2\}_2$ (**4**). **2** and **5** are the first examples of d^0 metallacarboranes incorporating a η^7-carboranyl ligand. All of these complexes have been fully characterized by various spectroscopic date, elemental analyses, and X-ray diffraction studies. Molecular orbital calculations indicate that the metal−carborane bonding is well delocalized and can be described as the orbital interactions between the metal's five d orbitals and the cage's five symmetry-adapted frontier orbitals. It is anticipated that only the d^0/f^n transition metal ion with the proper size is capable of being η^7-bound to an *arachno*-carboranyl ligand.

Introduction

The chemistry of metallacarboranes has witnessed an explosive growth since the first metallacarborane was reported in 1965.[1,2] A large number of metallacarboranes of s-, p-, d-, and f-block elements are known; however, the highest hapticity of carboranyl ligands in these compounds has been six until our recent report on an unprecedented mixed-sandwich compound $[\{(\eta^7\text{-}C_2B_{10}H_{12})(\eta^6\text{-}C_2B_{10}H_{12})U\}\{K_2(THF)_5\}]_2$ in which the U atom is η^7-bound to one of the $C_2B_{10}H_{12}$ ligands.[3] This is a brand new bonding mode for carborane molecules, and it is totally unexpected since it has been reported that interaction of a 13-vertex *closo*-metallacarborane $(\eta^6\text{-}C_2B_{10}H_{12})Co(\eta^5\text{-}C_5H_5)$ with Na/naphthalene followed by treatment with C_5H_5Na and $CoCl_2$ gave a 14-vertex *closo*-metallacarborane $[(\eta^6{:}\eta^6\text{-}C_2B_{10}H_{12})\text{-}\{Co(\eta^5\text{-}C_5H_5)\}_2]$ with the proposed geometry of a bicapped hexagonal antiprism.[4] Although the X-ray confirmation of this species has not been reported, successful structural characterization of another 14-vertex *closo*-metallacarborane $[\{\eta^6{:}\eta^6\text{-}(CH_3)_4C_4B_8H_8\}\{Fe(\eta^5\text{-}C_5H_5)\}_2]$ has indicated that the bicapped hexagonal antiprism species is indeed the thermodynamically favored form.[5] We have very recently communicated another example of a lanthanacarborane bearing a η^7-carboranyl ligand.[6] The results show that the metal−carbon(cage) distances are significantly shorter than those in other metallacarboranes, and are at the short end of the corresponding metal−carbon σ bonds. We are wondering if this type of bonding mode is only limited to f-block transition metals. To better understand the bonding interaction between metal ion and η^7-carborane anion and to facilitate the theoretical calculations, we have extended our research to d^0 transition metal. Yttrium was chosen because its properties are similar to those of lanthanide series in terms of the ionic radium, oxidation state, and chemical reactions.[7] Furthermore, Y^{3+} is a diamagnetic species, which benefits NMR measurements. On the other hand, to eliminate the ambiguity and to definitely distinguish the cage carbon atoms from those boron atoms of the carborane molecule in X-ray diffraction studies, a carbon-substituted *o*-carborane, 1,2-$(C_6H_5CH_2)_2$-1,2-$C_2B_{10}H_{10}$, was then chosen as a ligand. We report herein an experimental/theoretical study on d^0/f^n metallacarboranes bearing a η^7-$C_2B_{10}H_{10}R_2^{4-}$ ligand. The effects of the central metal ions, solvents, and alkali metal ions on the molecular structures of metallacarboranes are also discussed.

Experimental Section

General Procedures. All experiments were preformed under an atmosphere of dry dinitrogen with the rigid exclusion of air and moisture, using standard Schlenk or cannula techniques, or in a

[†] The Chinese University of Hong Kong.

[‡] The Hong Kong University of Science and Technology.

(1) Hawthorne, M. F.; Young, D. C.; Wegner, P. A. *J. Am. Chem. Soc.* **1965**, *87*, 1818.

(2) For recent reviews, see: (a) Grimes, R. N. In *Comprehensive Organometallic Chemistry II*; Abel, E. W., Stone, F. A. G., Wilkinson, G., Eds.; Pergamon: Oxford, 1995; Vol. 1, p 371. (b) Saxena, A. K.; Hosmane, N. S. *Chem. Rev.* **1993**, *93*, 1081. (c) Saxena, A. K.; Maguire, J. A.; Hosmane, N. S. *Chem. Rev.* **1997**, *97*, 2421.

(3) Xie, Z.; Yan, C.; Yang, Q.; Mak, T. C. W. *Angew. Chem., Int. Ed.* **1999**, *38*, 1761.

(4) Evans, W. J.; Hawthorne, M. F. *J. Chem. Soc., Chem. Commun.* **1974**, 38.

(5) (a) Pipal, J. R.; Grimes, R. N. *Inorg. Chem.* **1978**, *17*, 6. (b) Maxwell, W. M.; Weiss, R.; Sinn, E.; Grimes, R. N. *J. Am. Chem. Soc.* **1977**, *99*, 4016.

(6) Xie, Z.; Chui, K.; Yang, Q.; Mak, T. C. W. *Organometallics* **1999**, *18*, 3947.

(7) For recent reviews, see: (a) Schumann, H.; Messe-Markscheffel, J. A.; Esser, L. *Chem. Rev.* **1995**, *95*, 865. (b) Edelmann, F. T. In *Comprehensive Organometallic Chemistry II*; Abel, E. W., Stone, F. A. G., Wilkinson, G., Eds.; Pergamon: New York, 1995; Vol. 4, p 11.

10.1021/ja000188m CCC: $19.00
Published on Web 06/02/2000

glovebox. All organic solvents (except CH_3CN) were freshly distilled from sodium benzophenone ketyl immediately prior to use. CH_3CN was freshly distilled from CaH_2 immediately prior to use. Anhydrous MCl_3[8] and 1,2-$(C_6H_5CH_2)_2$-1,2-$C_2B_{10}H_{10}$[9] were prepared according to the literature methods. All other chemicals were purchased from Aldrich Chemical Co. and used as received unless otherwise noted. Infrared spectra were obtained from KBr pellets prepared in the glovebox on a Perkin-Elmer 1600 Fourier transform spectrometer. ^{1}H and ^{13}C NMR spectra were recorded on a Bruker DPX 300 spectrometer at 300.13 and 75.47 MHz, respectively. ^{11}B NMR spectra were recorded on a Varian Inova 400 spectrometer at 128.32 MHz. All chemical shifts are reported in δ units with reference to internal or external TMS (0.00 ppm) or with respect to the residual protons of the deuterated solvent for proton and carbon chemical shifts and to external $BF_3 \cdot OEt_2$ (0.00 ppm) for boron chemical shifts. Elemental analyses were performed by MEDAC Ltd, Brunel University, Middlesex, U.K.

Preparation of $\{[(C_6H_5CH_2)_2C_2B_{10}H_{10}]Dy(THF)\}_2\{Na(THF)_3\}_2 \cdot 2THF$ (1). A THF solution (20 mL) of 1,2-$(C_6H_5CH_2)_2$-1,2-$C_2B_{10}H_{10}$ (0.20 g, 0.62 mmol) was added to a suspension of Na metal (0.10 g, 4.35 mmol) in THF (10 mL) at room temperature, and the mixture was stirred at room temperature overnight. After addition of $DyCl_3$ (0.17 g, 0.63 mmol), the reaction mixture was refluxed with stirring for 4 days. The precipitate and excess Na metal were filtered off and washed with THF (8 mL × 3). The THF solutions were then combined and concentrated under vacuum to about 15 mL. **1** was isolated as yellow crystals after this solution was left standing at room temperature for 5 days (0.41 g, 76%). ^{1}H NMR (pyridine-d_5): δ 4.57 (br s), 2.43 (br s) (THF), and other broad, unresolved resonances. ^{13}C NMR (pyridine-d_5): δ 65.8, 23.7 (THF); other carbon atoms were not observed. ^{11}B NMR (pyridine-d_5): δ −13.4 (v br). IR (KBr, cm^{-1}): ν 3066 (w), 2970 (s), 2876 (vs), 2616 (w), 2569 (m), 2475 (vs), 2424 (s), 2356 (m), 1599 (w), 1449 (m), 1381 (w), 1300 (w), 1166 (m), 1048 (vs), 904 (s), 810 (w), 746 (w), 702 (m), 608 (w), 530 (w). Anal. Calcd for $C_{64}H_{112}B_{20}Dy_2Na_2O_8$ (**1**−2THF): C, 48.14; H, 7.07. Found: C, 47.89; H, 7.32.

Preparation of $\{[(C_6H_5CH_2)_2C_2B_{10}H_{10}]Y(THF)\}_2\{Na(THF)_3\}_2 \cdot 2THF$ (2). This compound was prepared as yellow crystals from YCl_3 (0.12 g, 0.61 mmol), 1,2-$(C_6H_5CH_2)_2$-1,2-$C_2B_{10}H_{10}$ (0.20 g, 0.62 mmol), and Na metal (0.092 g, 4.0 mmol) in 30 mL of THF using the procedures used above for **1**. Yield: 0.26 g (53%). ^{1}H NMR (pyridine-d_5): δ 7.65 (d, J = 7.5 Hz, 4H, *o*-aryl H), 6.96 (t, J = 7.5 Hz, 4H, *m*-aryl H), 6.79 (t, J = 7.2 Hz, 2H, *p*-aryl H), 4.90 (d, J_{H-H} = 13.2 Hz, 2H, $C_6H_5CH_2$), 4.35 (d, J_{H-H} = 13.2 Hz, 2H, $C_6H_5CH_2$), 3.67 (m, 20H, THF), 1.64 (m, 20H, THF). ^{13}C NMR (pyridine-d_5): δ 146.4, 129.9, 127.1, 124.2, 50.6 (benzyl), 106.7 (d, J_{Y-C} = 20.8 Hz, cage C), 67.2, 25.2 (THF). ^{11}B NMR (pyridine-d_5): δ 0.53 (2B), −13.5 (2B), −17.4 (3B), −24.9 (2B), −34.4 (1B). IR (KBr, cm^{-1}): ν 3058 (w), 3018 (w), 2967 (s), 2873 (s), 2466 (vs), 2429 (vs), 2354 (s), 1599 (w), 1490 (m), 1450 (m), 1383 (w), 1260 (w), 1169 (m), 1048 (vs), 907 (m), 798 (m), 702 (m), 530 (w). Anal. Calcd for $C_{60}H_{104}B_{20}Na_2O_7Y_2$ (**2**−3THF): C, 52.31; H, 7.61. Found: C, 51.94; H, 7.66.

Preparation of $\{[(C_6H_5CH_2)_2C_2B_{10}H_{10}]Er(THF)\}_2\{Na(THF)_3\}_2 \cdot 2THF$ (3). This compound was prepared as pink crystals from $ErCl_3$ (0.17 g, 0.62 mmol), 1,2-$(C_6H_5CH_2)_2$-1,2-$C_2B_{10}H_{10}$ (0.20 g, 0.62 mmol), and Na metal (0.102 g, 4.4 mmol) in 30 mL of THF using the procedures used above for **1**. Yield: 0.28 g (52%). ^{1}H NMR (pyridine-d_5): δ 4.71 (br s), 3.04 (br s) (THF), and other broad, unresolved resonances. ^{13}C NMR (pyridine-d_5): δ 69.7, 27.9 (THF); other carbon atoms were not observed. ^{11}B NMR (pyridine-d_5): δ −21.9 (v br). IR (KBr, cm^{-1}): ν 3052 (w), 3026 (w), 2970 (s), 2872 (s), 2470 (vs), 2433 (vs), 2359 (s), 1601 (w), 1491 (m), 1449 (m), 1383 (m), 1259 (w), 1170 (m), 1048 (vs), 903 (m), 861 (m), 797 (m), 751 (m), 702 (m). Anal. Calcd for $C_{60}H_{104}B_{20}Er_2Na_2O_7$ (**3**−3THF): C, 46.97; H, 6.83. Found: C, 47.07; H, 7.26.

Preparation of $\{[(C_6H_5CH_2)_2C_2B_{10}H_{10}]Er(DME)\}_2\{Na(DME)_2\}_2$ (4). A THF solution (10 mL) of 1,2-$(C_6H_5CH_2)_2$-1,2-$C_2B_{10}H_{10}$ (0.20 g, 0.62 mmol) was added to a suspension of Na metal (0.086 g, 3.74 mmol) in THF (10 mL) at room temperature, and the mixture was stirred at room temperature overnight. After addition of a suspension of $ErCl_3$ (0.17 g, 0.62 mmol) in THF (10 mL), the reaction mixture was refluxed for 4 days. Removal of the solvent gave a red solid that was extracted with dimethoxyethane (DME) (10 mL × 2). The clear DME solutions were combined and concentrated to about 8 mL. **4** was isolated as orange crystals after this solution was left standing at room temperature for days (0.26 g, 54%). ^{1}H NMR (pyridine-d_5): many broad, unresolved resonances. ^{13}C NMR (pyridine-d_5): δ 112.5, 99.9 (DME); other carbon atoms were not observed. ^{11}B NMR (pyridine-d_5): δ 32.9 (8B), 20.0 (2B). IR (KBr, cm^{-1}): ν 3019 (w), 2892 (m), 2830 (m), 2460 (vs), 2400 (s), 2350 (m), 1597 (w), 1452 (m), 1379 (w), 1255 (w), 1188 (w), 1088 (vs), 1044 (s), 910 (w), 858 (m), 802 (w), 744 (w), 699 (m), 538 (w). Anal. Calcd for $C_{44}H_{78}B_{20}Er_2Na_2O_6$ (**4**−3DME): C, 40.65; H, 6.05. Found: C, 40.60; H, 6.36.

This compound can also be prepared by recrystallization of **3** from a DME solution.

Preparation of $[\{(C_6H_5CH_2)_2C_2B_{10}H_{10}\}Y(THF)]_2[Li(THF)_4]_2$ (5). To a suspension of Li metal (0.032 g, 4.57 mmol) in THF (10 mL) was added a THF solution (15 mL) of 1,2-$(C_6H_5CH_2)_2$-1,2-$C_2B_{10}H_{10}$ (0.20 g, 0.62 mmol) at room temperature, and the mixture was stirred for 2 h. After addition of YCl_3 (0.24 g, 1.22 mmol), the reaction mixture was stirred at room temperature for 4 days. During the course of reaction, a large amount of yellow precipitate was formed. This solid was collected and extracted with acetonitrile (10 mL × 3). Removal of the solvent gave a bright yellow powder (0.31 g, 64%). Recrystallization from a CH_3CN/THF solution at room temperature afforded X-ray quality crystals. ^{1}H NMR (pyridine-d_5): δ 7.72 (d, J = 7.2 Hz, 4H, *o*-aryl H), 6.94 (t, J = 7.5 Hz, 4H, *m*-aryl H), 6.73 (t, J = 7.5 Hz, 2H, *p*-aryl H), 5.04 (d, J_{H-H} = 12.9 Hz, 2H, $C_6H_5CH_2$), 4.40 (d, J_{H-H} = 12.9 Hz, 2H, $C_6H_5CH_2$), 3.63 (m, 20H, THF), 1.59 (m, 20H, THF). ^{13}C NMR (pyridine-d_5): δ 147.3, 130.3, 127.3, 124.3, 51.4 (benzyl), 113.0 (d, J_{Y-C} = 23.7 Hz, cage C), 67.5, 25.4 (THF). ^{11}B NMR (pyridine-d_5): δ 0.7 (2B), −12.8 (2B), −15.9 (3B), −23.7 (2B), −33.1 (1B). IR (KBr, cm^{-1}): ν 3059 (w), 3020 (w), 2967 (s), 2879 (s), 2462 (vs), 2361 (s), 1599 (w), 1488 (w), 1450 (m), 1383 (m), 1260 (w), 1168 (m), 1041 (vs), 887 (m), 801 (w), 749 (w), 702 (w), 605 (w), 532 (w). Anal. Calcd for $C_{64}H_{112}B_{20}Li_2O_8Y_2$ (**5**−2THF): C, 54.23; H, 7.96. Found: C, 54.37; H, 8.08.

Preparation of $[\{(C_6H_5CH_2)_2C_2B_{10}H_{10}\}Er(THF)]_2[Li(THF)_4]_2$ (6). This compound was prepared as orange red crystals from $ErCl_3$ (0.34 g, 1.23 mmol), Li metal (0.062 g, 8.86 mmol), and 1,2-$(C_6H_5CH_2)_2$-1,2-$C_2B_{10}H_{10}$ (0.20 g, 0.62 mmol) in 25 mL of THF using the procedures used above for **5**. Yield: 0.35 g (66%). ^{1}H NMR (pyridine-d_5): δ 4.89 (br s), 2.81 (br s) (THF), and other broad, unresolved resonances. ^{13}C NMR (pyridine-d_5): δ 69.4, 27.5; other carbon atoms were not observed. ^{11}B NMR (pyridine-d_5): δ −4.0 (8B), −20.1 (2B). IR (KBr, cm^{-1}): ν 3060 (w), 2966 (s), 2879 (m), 2459 (vs), 2370 (m), 2169 (w), 1592 (m), 1534 (w), 1490 (m), 1447 (m), 1252 (w), 1167 (m), 1038 (vs), 887 (m), 746 (w), 701 (w), 530 (w), 413 (w). Anal. Calcd for $C_{68}H_{120}B_{20}Er_2Li_2O_9$ (**6**−THF): C, 49.61; H, 7.35. Found: C, 49.36; H, 7.31.

Computational Detail. Density functional calculations at the B3LYP level were performed on the model complex $[(\eta^7\text{-}C_2B_{10}H_{12})Y(H_2O)]_2^{2-}$ on the basis of the experimentally determined geometry. In the model complex, the benzyl substituents were replaced by hydrogen atoms and the coordinated THF ligand was simplified to H_2O for theoretical simplicity. The basis set used for C, B, O, and H was 6-31G while an effective core potential with a LanL2DZ basis set was employed for Y.[10] All calculations were carried out using the Gaussian 98 package[11] on Pentium III (550 MHz) computers. Natural Bond Order (NBO) analyses were also performed using the NBO program[12] as implemented in the Gaussian 98 package. The molecular orbitals obtained from

(8) Taylor, M. D.; Carter, C. P. *J. Inorg. Nucl. Chem.* **1962**, *24*, 387.
(9) Xie, Z.; Liu, Z.; Chiu, K.-Y.; Xue, F.; Mak, T. C. W. *Organometallics* **1997**, *16*, 2460.
(10) Hay, P. J.; Wadt, W. R. *J. Chem. Phys.* **1985**, *82*, 299.
(11) Frisch, M. J.; Trucks, G. W.; Schlegel, H. B.; Scuseria, G. E.; Robb, M. A.; Cheeseman, J. R.; Zakrzewski, V. G.; Montgomery, J. A., Jr.; Stratmann, R. E.; Burant, J. C.; Dapprich, S.; Millam, J. M.; Daniels, A. D.; Kudin, K. N.; Strain, M. C.; Farkas, O.; Tomasi, J.; Barone, V.; Cossi, M.; Cammi, R.; Mennucci, B.; Pomelli, C.; Adamo, C.; Clifford, S.; Ochterski, J.; Petersson, G. A.; Ayala, P. Y.; Cui, Q.; Morokuma, K.; Malick, D. K.; Rabuck, A. D.; Raghavachari, K.; Foresman, J. B.; Cioslowski, J.; Ortiz, J. V.; Stefanov, B. B.; Liu, G.; Liashenko, A.; Piskorz, P.; Komaromi, I.; Gomperts, R.; Martin, R. L.; Fox, D. J.; Keith, T.; Al-Laham, M. A.;

Table 1. Crystal Data and Summary of Data Collection and Refinement for **1**−**6**

	1	**2**	**3**	**4**	**5**	**6**
formula	$C_{36}H_{64}B_{10}DyNaO_5$	$C_{36}H_{64}B_{10}NaO_5Y$	$C_{36}H_{64}B_{10}ErNaO_5$	$C_{28}H_{54}B_{10}ErNaO_6$	$C_{36}H_{64}B_{10}LiO_5Y$	$C_{36}H_{64}B_{10}ErLiO_5$
crystal size (mm)	0.56 × 0.40 × 0.26	0.45 × 0.42 × 0.40	0.50 × 0.30 × 0.30	0.44 × 0.20 × 0.08	0.40 × 0.35 × 0.30	0.45 × 0.26 × 0.24
fw	870.5	796.9	875.2	785.1	780.8	859.2
crystal system	monoclinic	monoclinic	monoclinic	triclinic	monoclinic	monoclinic
space group	$P2_1/n$	$P2_1/n$	$P2_1/n$	$P\bar{1}$	$P2_1/n$	$P2_1/n$
a, Å	16.315(1)	16.354(2)	16.315(1)	9.597(1)	16.724(3)	16.724(3)
b, Å	14.444(1)	14.331(2)	14.444(1)	14.867(3)	14.249(3)	14.225(3)
c, Å	19.452(1)	19.469(3)	19.452(1)	16.246(3)	18.530(4)	18.483(4)
α, deg	90.00	90.00	90.00	114.37(1)	90.00	90.00
β, deg	105.52(1)	105.59(1)	105.52(1)	102.23(1)	103.83(3)	103.95(3)
γ, deg	90.00	90.00	90.00	90.44(1)	90.00	90.00
V, Å^3	4417(1)	4395(1)	4417(1)	2052(1)	4288(1)	4272(2)
Z	4	4	4	2	4	4
D_{calcd}, Mg/m^3	1.308	1.203	1.315	1.271	1.210	1.336
radiation (*λ*), Å	Mo Kα (0.71073)	Mo Kα (0.71073)	Mo Kα (0.71073)	Mo Kα (0.71073)	Mo Kα (0.71073)	Mo Kα (0.71073)
2*θ* range, deg	3.6 to 50.0	3.6 to 50.0	4.0 to 51.2	2.8 to 50.0	3.6 to 51.2	2.9 to 50.0
μ, mm^{-1}	1.739	1.374	1.947	2.089	1.398	2.002
F(000)	1788	1680	1796	798	1648	1764
no. of indep reflns	6983	5920	7592	5941	6409	6571
no. of obsd reflns	6412	5920	7040	5470	6409	6571
no. of params refnd	486	479	486	428	479	518
goodness of fit	1.068	1.100	1.040	1.028	1.168	1.077
*R*1	0.054	0.076	0.045	0.066	0.087	0.048
*wR*2	0.140	0.202	0.137	0.171	0.162	0.124

Table 2. Selected Bond Lengths (Å)

	1 (M = Dy)	**2** (M = Y)	**3** (M = Er)	**4** (M = Er)	**5** (M = Y)	**6** (M = Er)
M−C1	2.394(3)	2.408(3)	2.384(2)	2.414(3)	2.392(2)	2.375(5)
M−C2	2.382(2)	2.375(2)	2.348(2)	2.390(3)	2.362(3)	2.343(5)
M−B3	2.634(3)	2.619(3)	2.610(2)	2.693(3)	2.625(3)	2.617(6)
M−B4	2.643(3)	2.626(3)	2.620(2)	2.694(4)	2.640(3)	2.605(5)
M−B5	2.690(2)	2.700(2)	2.668(2)	2.697(4)	2.686(2)	2.711(6)
M−B6	2.745(2)	2.744(2)	2.713(2)	2.645(5)	2.732(3)	2.724(6)
M−B7	2.729(2)	2.737(3)	2.713(2)	2.670(4)	2.743(3)	2.677(7)
M−O	2.374(2)	2.352(2)	2.341(1)	2.511(3)	2.353(2)	2.343(4)
M···B5A	2.869(3)	2.836(3)	2.829(2)	2.837(4)	2.849(3)	2.818(5)
M···B6A	2.783(3)	2.789(3)	2.758(2)	2.827(4)	2.797(3)	2.780(6)
M−H5A	2.28(3)	2.25(3)	2.25(3)	2.19(3)	2.25(3)	2.24(3)
M−H6A	2.09(3)	2.10(3)	2.07(3)	2.10(3)	2.11(3)	2.13(3)

B3LYP results were plotted using the Molden v3.5 program written by G. Schaftenaar.[13]

X-ray Structure Determination. All single crystals were immersed in Paraton-N oil and sealed under N_2 in thin-walled glass capillaries. Data were collected at 293 K on an MSC/Rigaku RAXIS-IIC imaging plate using Mo Kα radiation from a Rigaku rotating-anode X-ray generator operating at 50 kV and 90 mA. An absorption correction was applied by correlation of symmetry-equivalent reflections using the ABSCOR program.[14] All structures were solved by direct methods and subsequent Fourier difference techniques and refined anisotropically for all non-hydrogen atoms by full-matrix least-squares calculations on F^2 using the Siemens SHELXTL program package (PC version).[15] Most of the carborane hydrogen atoms were located from different Fourier syntheses. All other hydrogen atoms were geometrically fixed using the riding model. One of the four coordinated THF molecules (C51−C54) in $[Li(THF)_4]^+$ moieties of both **5** and **6** is disordered over two sets of positions with 0.5:0.5 occupancies. Crystal data and details of data collection and structure refinement are given in Table 1. Selected bond distances are listed in Table 2. Further details are included in the Supporting Information.

Results and Discussion

Synthesis. We have previously reported that 1,2-$(C_6H_5CH_2)_2$-1,2-$C_2B_{10}H_{10}$ can be reduced by Na or K metal to generate [*nido*-$(C_6H_5CH_2)_2C_2B_{10}H_{10}]^{2-}$ which is capable of being *σ*- and η^6-bound to lanthanide ions affording *exo-nido*- and *closo*-lanthanacarboranes, respectively.[16] Treatment of 1,2-$(C_6H_5CH_2)_2$-1,2-$C_2B_{10}H_{10}$ with excess Na metal in THF followed by reaction with 1 equiv of MCl_3 in the presence of excess Na metal at reflux temperature gave novel 13-vertex *closo*-metallacarboranes of the general formula $\{[(C_6H_5CH_2)_2C_2B_{10}H_{10}]M(THF)\}_2\{Na(THF)_3\}_2\cdot 2THF$ (M = Dy (**1**), Y (**2**), Er (**3**)) in moderate to good yield (Scheme 1). The coordinated THF molecules in these metallacarboranes can be replaced by dimethoxyethane (DME) molecules giving $\{[(C_6H_5CH_2)_2C_2B_{10}H_{10}]Er(DME)\}_2\{Na(DME)_2\}_2$ (**4**) if recrystallized from **3** from a DME solution. Since 1,2-$(C_6H_5CH_2)_2$-1,2-$C_2B_{10}H_{10}$ cannot be directly converted into the [*arachno*-$(C_6H_5CH_2)_2C_2B_{10}H_{10}]^{4-}$ by Na metal, it is reasonable to suggest that the 13-vertex *closo*-metallacarborane [η^6-$(C_6H_5CH_2)_2C_2B_{10}H_{10}$]-$MCl(THF)_x$ may serve as an intermediate that accepts two more electrons from Na metal to form the final product.

Peng, C. Y.; Nanayakkara, A.; Gonzalez, C.; Challacombe, M.; Gill, P. M. W.; Johnson, B.; Chen, W.; Wong, M. W.; Andres, J. L.; Gonzalez, C.; Head-Gordon, M.; Replogle, E. S.; Pople, J. A.; *Gaussian 98 (Revision A.5)*; Gaussian, Inc.: Pittsburgh, PA, 1998.

(12) Glendening, E. D.; Reed, A. E.; Carpenter, J. E.; Weinhold, F. NBO version 3.1.

(13) Schaftenaar, G. Molden v3.5, CAOS/CAMM Center Nijmegen, Toernooiveld, Nijmegen, The Netherlands, 1999.

(14) Higashi, T. ABSCOR−An Empirical Absorption Correction Based on Fourier Coefficient Fitting; Rigaku Corp.: Tokyo, 1995.

(15) SHELXTL V 5.03 Program Package; Siemens Analytical X-ray Instruments, Inc.: Madison, WI, 1995.

(16) Xie, Z.; Liu, Z.; Yang, Q.; Mak, T. C. W. *Organometallics* **1999**, *18*, 3603.

Scheme 1

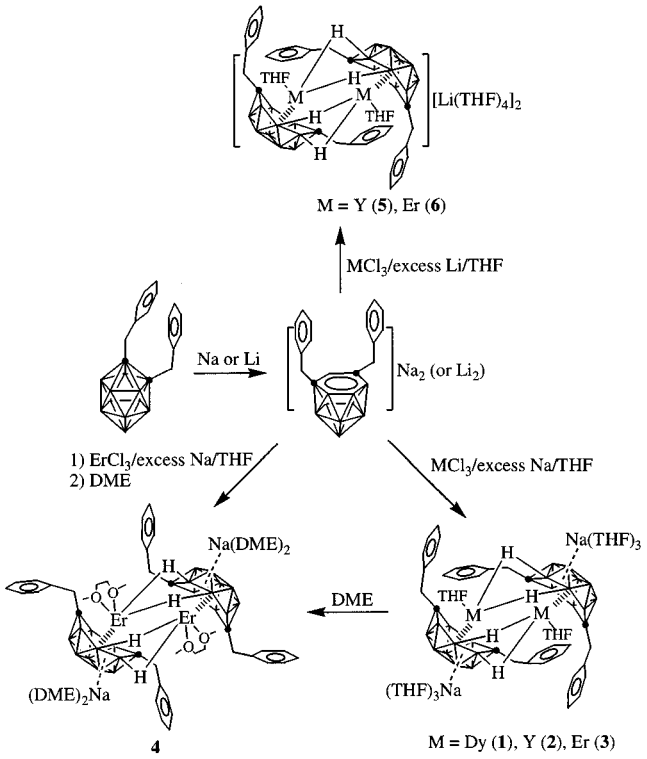

To study effects of alkali metal on the reactions and on the molecular structures of the resulting metallacarboranes, Li reduction reactions were examined. Under the same reaction conditions as mentioned above, only powdered solid containing chloride ions was isolated, which probably implies that LiCl cannot be completely removed from the product. After many experiments, we have found that excess MCl_3 can decrease the solubility of the resulting metallacarborane in the reaction mixture; on the other hand, the remaining MCl_3 can form a THF-soluble adduct $MCl_3 \cdot LiCl \cdot n$THF with LiCl in THF,[17] which allows the isolation of LiCl-free metallacarborane from the reaction mixture. Treatment of 1,2-$(C_6H_5CH_2)_2$-1,2-$C_2B_{10}H_{10}$ with excess Li metal followed by reaction with 2 equiv of MCl_3 at room temperature gave a large amount of precipitate that was recrystallized from a CH_3CN/THF solution to afford ionic compounds of the general formula $[\{(C_6H_5CH_2)_2C_2B_{10}H_{10}\}M(THF)]_2[Li(THF)_4]_2$ (M = Y (**5**), Er (**6**)) in moderate yield. The above transformations are summarized in Scheme 1.

These metallacarboranes (**1**−**6**) are all soluble in polar organic solvents such as THF, DME, pyridine, and CH_3CN, but insoluble in hexane. They have been fully characterized by various spectroscopic data, elemental analyses, and X-ray diffraction studies.

The IR spectra of **1**−**4** show a similar pattern for B−H absorption, a very strong peak at ∼2470 cm^{-1}, a strong peak at ∼2425 cm^{-1}, and a medium strong peak at ∼2355 cm^{-1}, which imply different types of B−H−M interactions.[18,19] The B−H splitting patterns in the IR spectra of **5** and **6** are very similar, exhibiting a very strong absorption at ∼2460 cm^{-1} and a medium strong peak at ∼2365 cm^{-1}, which are simpler than those of **1**−**4**, probably indicating that they have different types of B−H−M interactions.

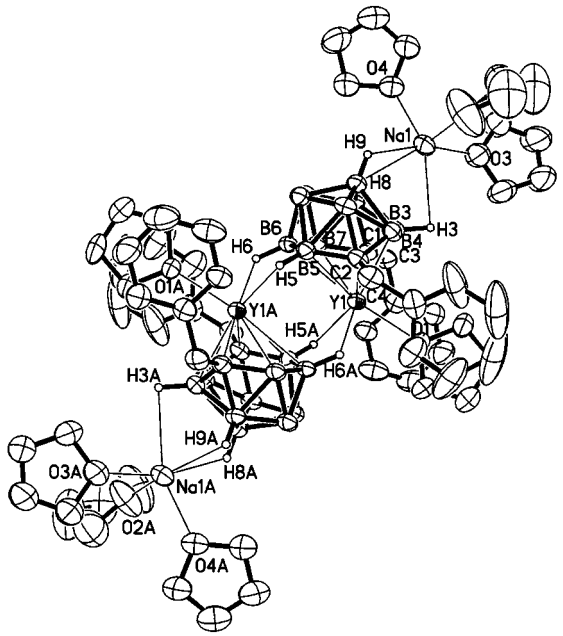

Figure 1. Molecular structure of $\{[(C_6H_5CH_2)_2C_2B_{10}H_{10}]Y(THF)\}_2\{Na(THF)_3\}_2 \cdot 2THF$ (**2**) (the solvated THF molecules are not shown; thermal ellipsoids are drawn at the 35% probability level).

The NMR spectra of metallacarboranes of Dy and Er are not very informative due to the strong paramagnetism of Dy^{3+} (μ_{eff} = 10.6 μ_B) and Er^{3+} (μ_{eff} = 9.5 μ_B).[20] The diamagnetic Y compounds, **2** and **5**, gave very nice NMR spectra. The ^{1}H NMR spectra support the ratio of five THF molecules per carboranyl ligand in these metallacarboranes, and indicate that the two methylene protons of the benzyl group are nonequivalent with the chemical shifts of ∼5.0 and ∼4.35 ppm, respectively. The proton-decoupled ^{13}C NMR spectra show a unique doublet at about 106.7 ppm with J_{Y-C} = 20.8 Hz, which is attributable to the cage carbon atoms.[21] The ^{11}B NMR spectra exhibit a 2:2:3:2:1 splitting pattern with the chemical shifts ranging from 0.5 to −35.0 ppm.

Structure. The solid-state structures of metallacarboranes **1**−**3** as derived from single-crystal X-ray analyses reveal that they are isomorphous and isostructural, and exhibit two THF of solvation. Figure 1 shows their representative structure. Each structure contains two $\{[\eta^7\text{-}(C_6H_5CH_2)_2C_2B_{10}H_{10}]M(THF)\}^-$ structural motifs that are connected by two sets of two B−H−M bonds, forming a centrosymmetrical dimer. Each central metal ion is η^7-bound to [*arachno*-$(C_6H_5CH_2)_2C_2B_{10}H_{10}]^{4-}$ and σ-bound to two B−H bonds from the neighboring [*arachno*-$(C_6H_5CH_2)_2C_2B_{10}H_{10}]^{4-}$ ligand and one oxygen atom of the THF molecule in a highly distorted-tetrahedral geometry with a formal coordination number of 8. The closest approach of M^{3+} to benzyl groups is greater than 3.7 Å, which indicates there are no obvious interactions between M^{3+} and benzyl substitu-

(17) Shen, Q.; Chen, W.; Jin, Y.; Shan, C. *Pure Appl. Chem.* **1988**, *60*, 1251.

(18) (a) Xie, Z.; Wang, S.; Zhou, Z.-Y.; Xue, F.; Mak, T. C. W. *Organometallics* **1998**, *17*, 489. (b) Xie, Z.; Wang, S.; Zhou, Z.-Y.; Mak, T. C. W. *Organometallics* **1998**, *17*, 1907. (c) Xie, Z.; Wang, S.; Zhou, Z.-Y.; Mak, T. C. W. *Organometallics* **1999**, *18*, 1641. (d) Xie, Z.; Wang, S.; Yang, Q.; Mak, T. C. W. *Organometallics* **1999**, *18*, 2420. (e) Wang, S.; Yang, Q.; Mak, T. C. W.; Xie, Z. *Organometallics* **1999**, *18*, 4478. (f) Wang, S.; Yang, Q.; Mak, T. C. W.; Xie, Z. *Organometallics* **1999**, *18*, 1578.

(19) (a) Khattar, R.; Knobler, C. B.; Hawthorne, M. F. *Inorg. Chem.* **1990**, *29*, 2191. (b) Khattar, R.; Knobler, C. B.; Hawthorne, M. F. *J. Am. Chem. Soc.* **1990**, *112*, 4962.

(20) Cotton, S. *Lanthanides and Actinides*; Oxford University Press: New York, 1991; p 11.

(21) (a) Hosmane, N. S.; Zhu, D.; Zhang, H.; Oki, A. R.; Maguire, J. A. *Organometallics* **1998**, *17*, 3196. (b) Schumann, H.; Erbstein, F.; Weimann, R.; Demtschuk, J. *J. Organomet. Chem.* **1997**, *536/7*, 541. (c) Schumann, H.; Rosenthal, E. C. E.; Kociok-Köhn, G.; Molander, G. A.; Winterfeld, J. *J. Organomet. Chem.* **1995**, *496*, 233.

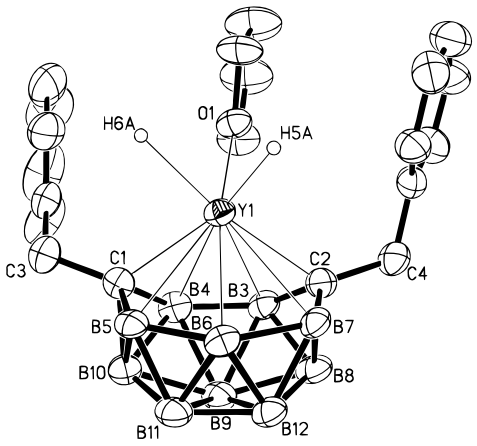

Figure 2. Closer view of the coordination environment for the Y atom in **2**.

ents.[16,22] As far as we are aware, **2** is the first metallacarborane of d-transition metal incorporating a η^7-carboranyl ligand to be reported.

Like the carboranyl ligand in $[\{(\eta^7\text{-}C_2B_{10}H_{12})(\eta^6\text{-}C_2B_{10}H_{12})U\}\{K_2(THF)_5\}]_2$[3] and $[\{[\eta^5{:}\eta^7\text{-}Me_2C(C_5H_4)(C_2B_{10}H_{11})]Er\}_2\{Na_4(THF)_9\}]_n$,[6] the [*arachno*-$(C_6H_5CH_2)_2C_2B_{10}H_{10}]^{4-}$ has a boatlike C_2B_5 bonding face in which the five B atoms are coplanar and the two C atoms are ca. 0.6 Å above this plane, resulting in significantly shorter M−C(cage) distances (Figure 2). Such a unique arrangement of the cage atoms leads to three different types of coordination environment for cage atoms: 5-coordinate carbon, 6-coordinate boron, and 7-coordinate boron, respectively.

The average M−C(cage) distances are 2.388(3) Å for **1**, 2.392(3) Å for **2**, and 2.366(2) Å for **3**, respectively. The differences in these distances are consistent with those in their Shannon's ionic radii.[23] It is noteworthy that these measured values are all at the short end of the relevant M−C σ bond distances.[24] For example, the average Y−C(cage) distance of 2.392(3) Å in **2** compares with the 2.362(11) Å in $(C_5H_5)_2YMe(THF)$,[25] 2.425(23) Å in $[(C_5H_5)_2Y(CH_2SiMe_3)_2]^-$,[26] 2.58(3) Å in $(C_5H_5)_2Y(\mu\text{-}Me_2)AlMe_2$,[27] 2.545(11) Å in $[(C_5H_5)_2Y(\mu\text{-}Me)]_2$,[28] 2.508 Å in $Y[(\mu\text{-}Me_2)AlMe_2]_3$,[29] 2.38(2) Å in $(C_5Me_5)_2Y(C{\equiv}CBu^t)_2Li(THF)$,[30] 2.468(7) Å in $(C_5Me_5)_2Y[CH(SiMe_3)_2]$,[31] 2.44(2) Å in $(C_5Me_5)_2YCH_3(THF)$,[32] and 2.418(6) Å in $Me_2Si(C_5Me_4)_2Y[CH(SiMe_3)_2]$,[33] but is significantly shorter than those of Y−C(cage) distances normally observed in yttracarboranes,[2b] for example, 2.649(16) Å in $\{[(SiMe_3)_2C_2B_4H_4]YCl_3\}^{2-}$,[21a] 2.728(17) Å in $\{[(SiMe_3)_2C_2B_4H_4]_2YCl(THF)\}^{2-}$,[21a] and 2.930(19) Å in $\{[(SiMe_3)_2C_2B_4H_4]_2Y(THF)\}^-$.[21a]

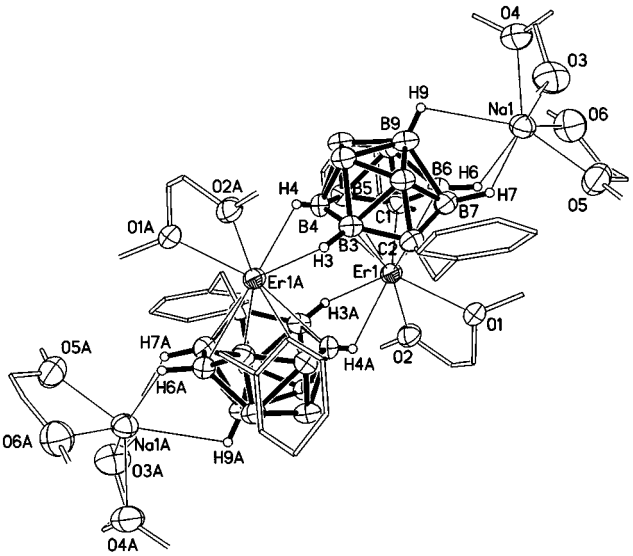

Figure 3. Molecular structure of $\{[(C_6H_5CH_2)_2C_2B_{10}H_{10}]Er(DME)\}_2\{Na(DME)_2\}_2$ (**4**) (thermal ellipsoids are drawn at the 35% probability level).

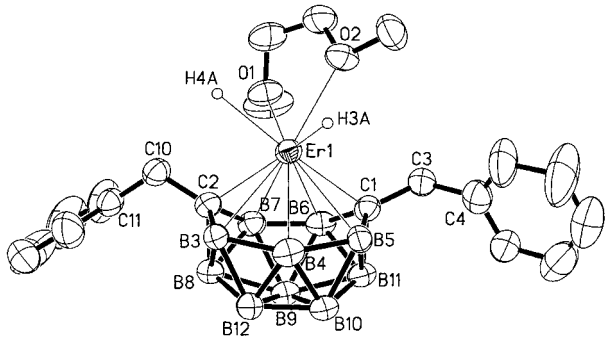

Figure 4. Closer view of the coordination environment for the Er atom in **4**.

Substitution of the coordinated THF molecules in **3** by the bidentate DME molecules resulted in the formation of a new metallacarborane **4**. X-ray analyses reveal that **4** is a centrosymmetric dimer consisting of two $\{[\eta^7\text{-}(C_6H_5CH_2)_2C_2B_{10}H_{10}]Er(DME)\}^-$ structural motifs that are connected by two sets of two B−H−Er bonds, a pattern which is similar to that in **3** (Figure 3). Each Er^{3+} ion is η^7-bound to [*arachno*-$(C_6H_5CH_2)_2C_2B_{10}H_{10}]^{4-}$ and σ-bound to two B−H bonds from the neighboring [*arachno*-$(C_6H_5CH_2)_2C_2B_{10}H_{10}]^{4-}$ ligand and two oxygen atoms of the DME molecule in a highly distorted-square-pyramidal geometry with a formal coordination number of 9. The bidentate DME molecule needs more coordination space than a monodentate THF ligand, which forces the changes in the orientation of the two benzyl substituents (Figure 4). Due to the higher coordination number of the central metal ion, the Er−C, Er−B, and Er−O distances in **4** are all slightly longer than the corresponding values in **3** (Table 2).

Replacement of the Na^+ ions in **2** and **3** by Li^+ ions affords ionic complexes **5** and **6**, respectively. X-ray diffraction studies show that **5** and **6** are isomorphous and isostructural. Figure 5 shows their representative structure. They are centrosymmetrical dimers consisting of alternating layers of discrete cations $[Li(THF)_4]^+$ and anions $\{[\eta^7\text{-}(C_6H_5CH_2)_2C_2B_{10}H_{10}]M(THF)\}_2^{2-}$. The coordination environment of the central metal ion is identical with that in **2** or **3** although they have different alkali ion complexes. It is not clear why Li^+ and Na^+ ions adopt a very different coordination mode. The molecular structure of

(22) Evans, W. J.; Seibel, C. A.; Ziller, J. W. *J. Am. Chem. Soc.* **1998**, *120*, 6745.
(23) Shannon, R. D. *Acta Crystallogr.* **1976**, *A32*, 751.
(24) Cotton, S. A. *Coord. Chem. Rev.* **1997**, *160*, 93.
(25) Evans, W. J.; Dominguez, R.; Hanusa, T. P. *Organometallics* **1982**, *5*, 263.
(26) Evans, W. J.; Dominguez, R.; Levan, K. R.; Doedens, R. J. *Organometallics* **1985**, *4*, 1837.
(27) Scollary, G. R. *Aust. J. Chem.* **1978**, *31*, 411.
(28) Holton, J.; Lappert, M. F.; Ballard, D. G. H.; Pearce, R.; Atwood, J. L.; Hunter, W. E. *J. Chem. Soc., Dalton Trans.* **1979**, 54.
(29) Evans, W. J.; Anwander, R.; Ziller, J. W. *Organometallics* **1995**, *14*, 1107.
(30) Evans, W. J.; Drummond, D. K.; Hanusa, T. P.; Olofson, J. M. *J. Organomet. Chem.* **1989**, *376*, 311.
(31) Den Haan, K. H.; De Boer, J. L.; Teuben, J. H.; Spek, A. L.; Kojic-Prodic, B.; Hays, G. R.; Huis, R. *Organometallics* **1986**, *5*, 1726.
(32) Den Haan, K. H.; De Boer, J. L.; Teuben, J. H.; Smeets, W. J. J.; Spek, A. L. *J. Organomet. Chem.* **1987**, *317*, 31.
(33) Jeske, G.; Schock, L. E.; Swepston, P. N.; Schumann, H.; Marks, T. J. *J. Am. Chem. Soc.* **1985**, *107*, 8103.

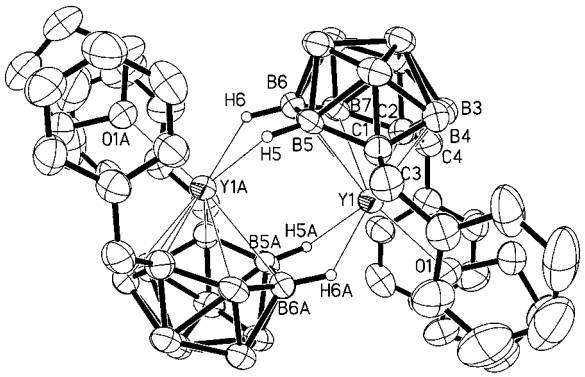

Figure 5. Molecular structure of $[\{(C_6H_5CH_2)_2C_2B_{10}H_{10}\}Y(THF)]_2^{2-}$ in **5** (thermal ellipsoids are drawn at the 35% probability level).

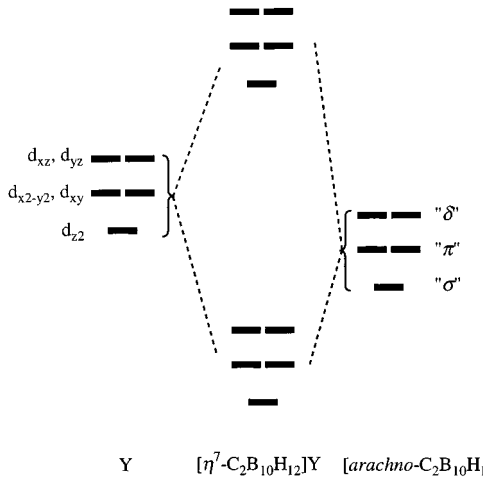

Figure 6. Schematic orbital interaction diagram showing the interactions between Y and the $[arachno\text{-}C_2B_{10}H_{12}]^{4-}$ cage fragment. Please see Figure 7 for the "σ", "π", and "δ" fragment orbitals of the cage. The Y to the center of the carborane cage is defined as the *z* axis.

the anion is very similar to that in metallacarboranes **1**−**3**. Therefore, the M−C, M−B, and M−O distances in **5** and **6** are very close to the corresponding values in **2** and **3**, respectively. For example, the average Er−C(cage) and Er−B(cage) distances of 2.359(5) and 2.667(6) Å in **6** compare with the 2.366(2) and 2.665(2) Å in **3** and the 2.385(4) and 2.656(5) Å in $[\{\eta^5{:}\eta^7\text{-}Me_2C(C_5H_4)(C_2B_{10}H_{11})\}Er_2(\mu\text{-}Cl)(THF)_3]_2$, respectively.[6]

Bonding. Our results have shown that d^0/f^n transition metal ions are capable of being η^7-bound to $[arachno\text{-}C_2B_{10}H_{10}R_2]^{4-}$ tetraanion forming a novel class of 13-vertex metallacarboranes. The arrangement of the cage atoms in these metallacarboranes is the same regardless of the substituents on the cage carbons and of d^0/f^n transition metal ions. To understand the bonding interactions between the metal ion and *arachno*-carboranyl ligand, molecular orbital calculations at the B3LYP level of the density functional theory have been performed on the model complex $[(\eta^7\text{-}C_2B_{10}H_{12})Y(H_2O)]_2^{2-}$, in which the benzyl substituents were replaced by H atoms and the coordinated THF molecule was simplified to H_2O for theoretical simplicity. Careful examination of the molecular orbitals obtained from the B3LYP calculations indicates that the metal's five d orbitals of Y are all significantly involved in the metal−$[\eta^7\text{-}C_2B_{10}H_{12}]$ bonding interactions. The relevant molecular orbitals are mainly found in the HOMO-LUMO region. A schematic molecular orbital interaction diagram based on the examination can be derived, shown in Figure 6. The five d orbitals of Y are arranged in the order of d_{z^2}, ($d_{x^2-y^2}$, d_{xy}), and (d_{xz}, d_{yz}) in the consideration

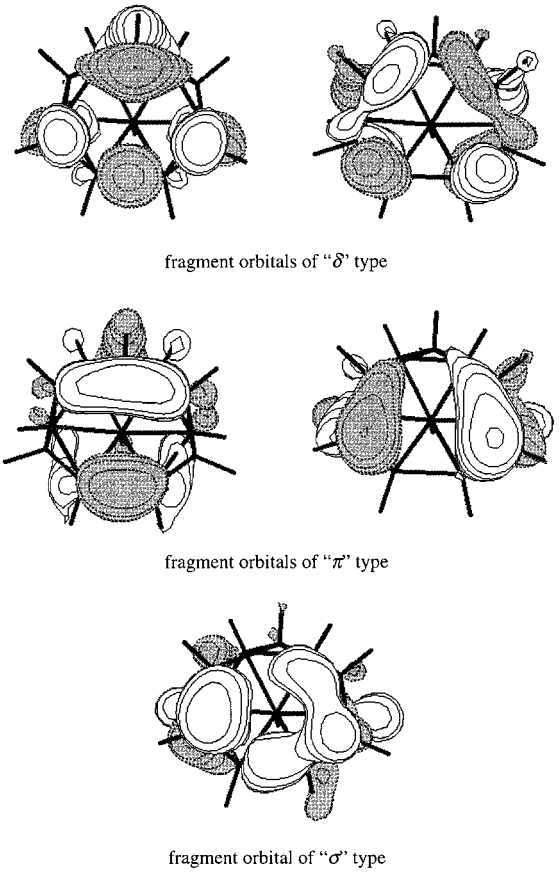

Figure 7. Frontier orbitals of the $[arachno\text{-}C_2B_{10}H_{12}]^{4-}$ tetraanion fragment.

of the ligand field given by the coordinated THF and B−H bonds from the neighboring carboranyl ligand. Calculations of the $[arachno\text{-}C_2B_{10}H_{12}]^{4-}$ tetraanion give five symmetry-adapted frontier fragment orbitals, shown in Figure 7, which can be classified as "σ", "π", and "δ" types depending on their nodal characteristics with respect to the metal−cage axis. The interactions between these two sets of molecular orbitals give rise to five bonding and five antibonding molecular orbitals. Clearly, the metal−cage interaction is extensively delocalized. In the more commonly observed metal−[η^5-carboranyl] complexes such as various $[(C_2B_9H_{11})_2M]^-$ or $[(C_2B_4H_4R_2)_2M]^-$, the η^5-carboranyl ligand is considered as a *nido* species and normally provides three pairs of electrons to the bonding with metal ions.[2] In the complexes dealt with in the current paper, the η^7-carboranyl ligand, $[C_2B_{10}H_{12}]^{4-}$, is formally taken as an *arachno* species, and an additional two pairs of electrons are involved in the metal−cage interactions as discussed in Figure 6.

The natural bond order (NBO)[34] analysis of $[arachno\text{-}C_2B_{10}H_{12}]^{4-}$ shows that in the boatlike C_2B_5 bonding face the natural atomic charges of carbons (av −0.85) are significantly higher than those of borons (av −0.16). The results are understandable because the carbons are more electronegative and less connected in the cage cluster. The results also imply that the carbons should form stronger bonds with the metal center. Indeed, the Wiberg bond orders from the NBO analysis[35] are much higher for the Y−C bonds (av 0.28) than those for the Y−B bonds (av 0.14). These results are in good agreement with the experimental data.

Calculations on the model complex show that the $[arachno\text{-}C_2B_{10}H_{12}]^{4-}$ tetraanion contributes five pairs of electrons to the

(34) Reed, A.; Curtiss, L. A.; Weinhold, F. *Chem. Rev.* **1988**, *88*, 899.
(35) Wiberg, K. B. *Tetrahedron* **1968**, *24*, 1083.

five d orbitals of the metal ion to form metal−cage bonds in η^7-fashion. It is anticipated that only d^0 and f-block transition metal ions with proper size can have such bonding interactions with the [*arachno*-$C_2B_{10}H_{12}]^{4-}$ ligand. This can explain why only 14-vertex *closo*-metallacarboranes with a bicapped hexagonal antiprism geometry, [(η^6:η^6-$C_2B_{10}H_{12}$){Co(η^5-C_5H_5)}$_2$][4] and [{η^6:η^6-$(CH_3)_4C_4B_8H_8$}{Fe(η^5-C_5H_5)}$_2$],[5] were isolated for Fe^{3+} (d^5) and Co^{3+} (d^6) ions. In other words, the [*arachno*-$C_2B_{10}H_{12}]^{4-}$ and [*arachno*-$(CH_3)_4C_4B_8H_8]^{4-}$ ligands cannot be stabilized by Fe^{3+} or Co^{3+} ions.

Conclusion. Several new 13-vertex *closo*-metallacarboranes of d^0/f^n transition metals bearing an η^7-carboranyl ligand have been prepared and structurally characterized. The isolation of the first d^0 yttracarborane is beneficial to the spectroscopic and theoretical studies. The substituents on cage carbons, solvents, and alkali metals can affect the overall molecular structures of the resulting complexes, or the coordination environment of the central metal ions, but have no effects on the basic structure of the 13-vertex metallacarborane structural motif.

The metal−carborane bonding in the studied complexes is well delocalized and can be described as the orbital interactions between the metal's five d orbitals and the cage's five symmetry-adapted frontier orbitals. These five frontier orbitals can be classified as one "σ", two "π", and two "δ" types, which are characteristics of an *arachno* structure, with respect to the metal−cage axis. The metal−carbon(cage) bonds are calculated to be much stronger than the metal−boron(cage) ones, which is consistent with experimental data. It is further anticipated that only d^0/f^n transition metal ions of the proper size are capable of being η^7-bound to an *arachno*-carboranyl ligand.

Acknowledgment. The work described in this paper was fully supported by a grant from the Research Grants Council of the Hong Kong Special Administration Region (Project No. CUHK 4210/99P).

Supporting Information Available: Tables of crystallographic data and data collection details, atomic coordinates, bond distances and angles, anisotropic thermal parameters, and hydrogen atom coordinates and figures giving atom-numbering schemes for metallacarboranes **1**−**6** (PDF). This material is available free of charge via the Internet at http://pubs.acs.org.

JA000188M